First-principles study of $Sn_2P_2Se_6$ ferroelectrics

Razvan Caracas and Xavier Gonze
Université Catholique de Louvain, Unité de Physico-Chimie et de Physique de Matériaux, pl. Croix du Sud 1, B-1348 Louvain-la-Neuve, Belgium
(Received 27 December 2001; published 27 September 2002)

We have investigated the electronic, structural, and dielectric properties of the ferroelectric $Sn_2P_2Se_6$ using the local density approximation of the density functional theory. The charge density analysis reveals the existence of isolated $[P_2Se_6]$ groups and Sn atoms, which are weakly bonded to each other. The band structure is made of weakly dispersive bands, which are assigned to different atomic and/or molecular orbitals. The electronic gap is on the order of ~ 1 eV. The theoretical determination of the structure underestimates the unit cell parameters (up to 6%) and the Sn-Se interatomic bond distances (up to 11%) with respect to the experimental results, while the agreement is excellent (within 1% for bond lengths) in the description of the $[P_2Se_6]$ group geometry. The Born effective charges of P and Se are much more anisotropic than those of Sn. The computed spontaneous polarization is on the order of 15 $\mu C\,cm^{-2}$.

DOI: 10.1103/PhysRevB.66.104106 PACS number(s): 71.20.Ps, 77.22.Ch, 77.22.Ej, 61.66.Fn

I. INTRODUCTION

$Sn_2P_2Se_6$ belongs to a large family of $A_2B_2C_6$ uniaxial displacive ferroelectrics, with $A=Sn,Pb,Cu,In$, $B=P$, and $C=S$, Se,[1–4] and is one of the few proper ferroelectrics that shows the presence of an incommensurately modulated phase, intermediate between the paraelectric and ferroelectric phases. The temperature range of stability of this incommensurate phase is (193–220 K). The high-temperature phase has symmetry $P2_1/c$ and the low-temperature phase has Pc symmetry.[3] Experimental data are available in the literature: phase transition analyses,[3,5,6] reports of Raman,[7,8] infrared,[7] and Mössbauer[9,10] spectroscopy, inelastic neutron scattering[11–13] experiments, thermal measurements,[14] memory effect analysis,[15] etc. The theoretical studies have focused up to now on the application of the dipole Ising model in order to understand the mechanisms governing the phase transitions and the appearance of the ferroelectricity.[16,17] We are not aware of first-principles calculations of the properties of $Sn_2P_2Se_6$. As concerns other members of the $A_2B_2C_6$ family, we are aware only of a Hartree-Fock study of $Sn_2P_2S_6$.[6]

In the present study we carry on such a first-principles investigation, dealing with the electronic, structural, and dielectric properties of the ferroelectric $Sn_2P_2Se_6$. For this we have used the local density approximation (LDA) of the density functional theory (DFT) (Refs. 18 and 19) as implemented in the ABINIT code.[20]

The paper is organized as follows. First the structure of the ferroelectric phase is briefly described (Sec. II); then details of the calculation method are presented (Sec. III). The valence charge density distribution and the electronic band structure are presented in Sec. IV. The *ab initio* determination of the crystal structure is discussed and compared to the experimental results in Sec. V, while the dielectric properties are reported in Sec. VI. Finally, we summarize this study.

II. CRYSTAL STRUCTURE

We considered the monoclinic ferroelectric phase using the Pc symmetry setting, with $a=6.8145$ Å, $b=7.7170$ Å, $c=11.692$ Å, and $\beta=124.549°$ as determined at 193 K.[21] There are 20 atoms in the unit cell. Equivalent pseudo-orthorhombic unit cell choices are also reported in the literature.[22]

Three-dimensional representations of the structure and of its corresponding Brillouin zone are shown in Fig. 1(a) and Fig. 1(b), respectively. With respect to basic chemical arguments and geometrical consideration, the structure may be seen as built of $[P_2Se_6]$ anionic groups and Sn cations. Within the $[P_2Se_6]$ group, each P atom is fourfold coordinated (one P atom and three Se atoms). A distance of 2.225 Å separates the two P atoms. The Se atoms are disposed at the apices of a basal triangle. The P-Se bond distance ranges between 2.18 and 2.20 Å . As a whole the group may be seen as a distorted trigonal antiprism, with monoclinic $2/m$ symmetry. The $[P_2Se_6]$ units are arranged along chains parallel to [010]. Two consecutive chains are in an antisymmetrical relationship. The Sn atoms lie between these $[P_2Se_6]$ units, surrounded by eight Se atoms at distances of 2.9 Å up to 3.6 Å, suggesting possible ionic-type bonds. They ensure the in-chain connections and the further binding of these chains in directions parallel to [100], [001], and [101].

III. COMPUTATIONAL DETAILS

All the calculations were based on the LDA of the DFT.[18,19] We used the ABINIT code, a common project of the Université Catholique de Louvain, Corning Incorporated and other contributors [ABINITv2, (Ref. 20)]. The ABINIT software is based on pseudopotentials and plane waves. It relies on the adaptation to a fixed potential of the band-by-band conjugate gradient method[23] and on a potential-based conjugate-gradient algorithm for the determination of the self-consistent potential.[24] As usual with plane-wave basis sets, the numerical accuracy of the calculation can be systematically improved by increasing the cutoff kinetic energy of the plane waves.

These wave functions describe only the valence and conduction electrons, while the core electrons are taken into ac-

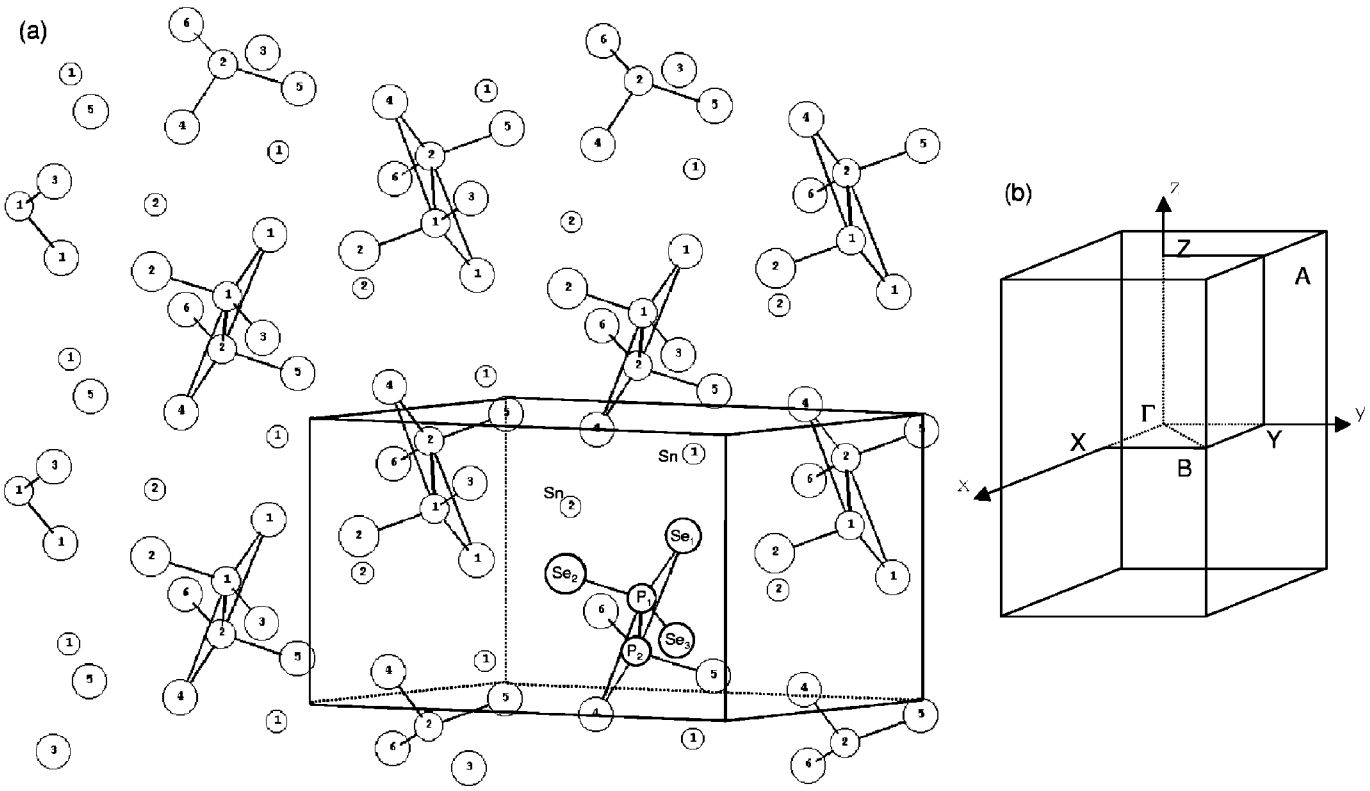

FIG. 1. Fragment of the crystal structure of $Sn_2P_2Se_6$ ferroelectrics (a) and its corresponding Brillouin zone (b). The P-Se and P-P bonds inside the $[P_2Se_6]$ group are shown. The atoms are, in decreasing size order, Se, P, and Sn. The numbers correspond to the different independent crystallographic sites. For the ease of the visualization, some of the atoms are labeled.

count using pseudopotentials. We used Troullier-Martins pseudopotentials[25] for the three elements, the core configuration for Sn being $[Kr]4d^{10}$, the one for P being [Ne], and the one for Se being $[Ar]3d^{10}$. The valence electrons shells were $5s^25p^2$, $3s^23p^3$, and $4s^24p^4$ for Sn, P, and Se, respectively.

For the characterization of the electronic properties a set of convergence tests has been done in order to choose correctly the grid of special **k** points[26] and the plane-wave kinetic energy cutoff. During these tests the grid density and the cutoff energy value have been consecutively and independently increased. The variation of the total energy has been monitored. A difference of 1 millihartrees (1 hartree $=27.211$ eV) between two successive grids and cutoff energies has been considered a good indication of the convergence. A regular $4\times4\times4$ grid of special **k** points, with 16 points in the irreducible part of the Brillouin zone, and a plane-wave kinetic energy cutoff of 26 hartrees have been finally adopted for the calculation of the electronic properties.

The structural relaxation was conducted using the Broyden-Fletcher-Goldfarb-Shanno minimization,[27] modified to take into account the total energy in addition to the gradients. Technical details on the computation of responses to atomic displacements and homogeneous electric fields can be found in Ref. 28, while Ref. 29 presents the subsequent computation of dynamical matrices, Born effective charges, dielectric permittivity tensors, and interatomic force constants.

IV. ELECTRONIC PROPERTIES

A. Valence charge density

We determine the electronic properties for the unrelaxed, experimental structure. The analysis of the valence charge distribution supports the empirical description of the structure, namely, the $[P_2Se_6]$ group, and almost isolated Sn cations. The isodensity lines in Fig. 2(a) display the main features of the P-P and P-Se bindings within this group. The electron density peaks lie around the Se, P, and Sn atoms at distances of about 0.7–0.85, 0.6–0.7, and 0.6–0.7 Å far from the respective atomic centers. There is a large amount of charge between the P atoms and in the PSe_3 tetrahedral regions. Along the P-P bond the minimum of the valence electron density represents about 94% of the P maximum peak, while along the P-Se this minimum represents 90% from the P maximum. The strength of the P-P bond induces a molecular behavior for the $[P_2Se_6]$ group.

A comparison between the P-Se and Sn-Se bonds, as seen in Fig. 2(b), shows much weaker Sn-Se bonds with mainly ionic character with a small covalent component.

B. Electronic band structure

The self-consistent calculation of the density of charge allows us to construct the LDA Kohn-Sham electronic band structure, represented in Fig. 3(a) along several special paths in the Brillouin zone. Directions parallel and perpendicular to the $[010]$ $[P_2Se_6]+Sn$ chains are illustrated. The elec-

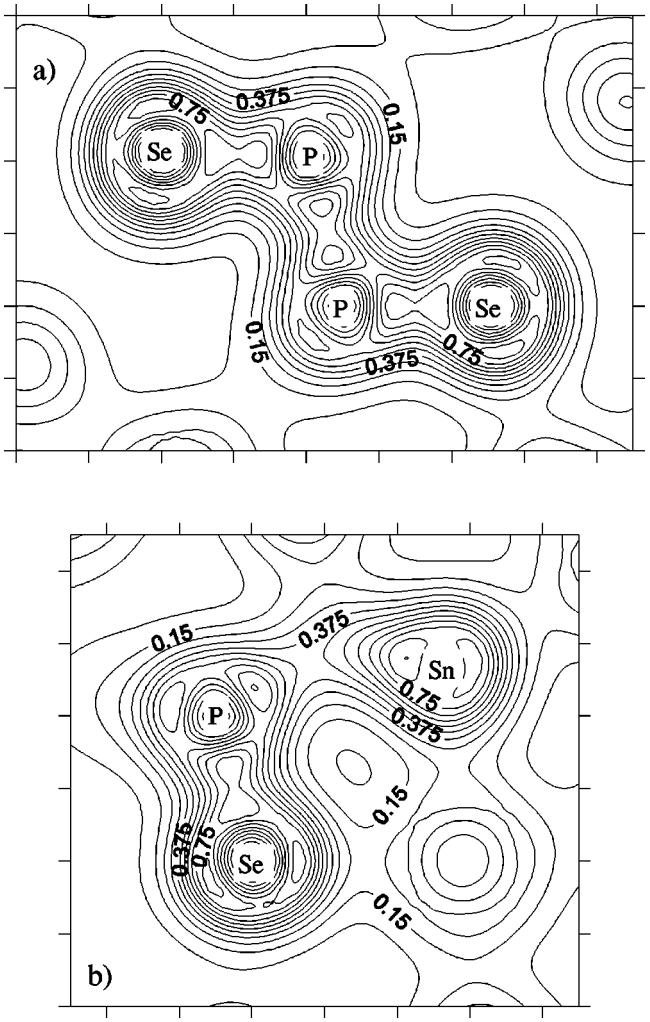

FIG. 2. Valence electron density distribution in $Sn_2P_2Se_6$. (a) Transverse cross section through the $[P_2Se_6]$ group. The P-P and P-Se bonds are clearly seen. (b) Cross section through P-Se-Sn atoms. The differences in the covalent character of the P-Se and Sn-Se bonds are clearly seen. Contour lines are separated by 0.075 $e/Å^3$. The side ticks are spaced by 2 bohrs.

tronic band structure is made of weakly dispersive bands, with no big differences between the paths.

We clearly see the separation of several groups of bands in the lower-energy region and the accumulation of flatbands in a 3.5 eV energy range just below the top of the valence bands. In the lower-energy region, the gaps between the different bands are up to 2 eV large. The nondispersive character of the band structure is less pronounced close to the Γ point, where for certain bands belonging to the same group a maximal splitting of 1 eV is observed.

The indirect (LDA Kohn-Sham) electronic gap is 0.9 eV.

C. Density of states

The electron density of states (DOS) as a function of the energy has been calculated from a $4\times4\times4$ **k**-point grid with a Gaussian smearing of 0.02 hartree. The DOS obtained for the valence and first conduction states is presented in Fig. 3(b). The peaks in the DOS correspond to the different

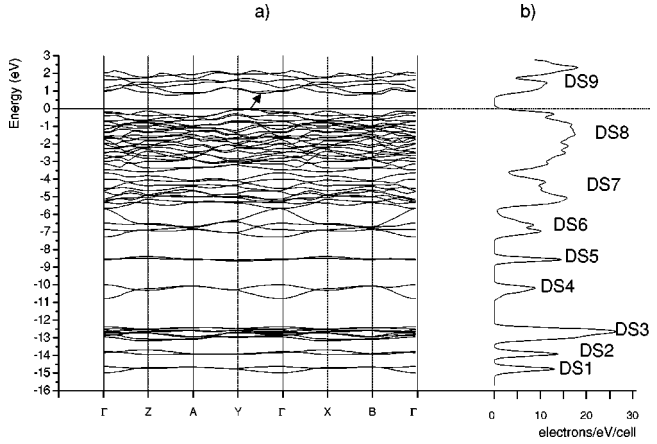

FIG. 3. Electron band structure (a) and the corresponding density of states (DOS) (b). The arrow indicates the indirect gap. The different labels correspond to the different groups of electronic bands. See the text for an analysis of the electronic charge belonging to these electronic bands.

groups of electronic bands. They are labeled $DS1$, $DS2,\ldots,DS10$. A partial valence electronic analysis was made in order to assign the charge belonging to the different peaks in the DOS to different atomic orbitals (AO's) and/or molecular orbitals (MO's).

D. Partial charge density

The charge densities corresponding to certain groups of electronic bands are represented in Fig. 4. A cross section passing through the Se-P-P-Se median plane of the $[P_2Se_6]$ group and another one passing through a P-Se-Sn plane are shown for several DS groups.

The $DS1$ up to $DS5$ charge stems mainly from the $[2P(3s)+6Se(4s)]$ MO. As there are two $[P_2Se_6]$ groups in the unit cell, the number of bands assigned to the $[2P+6Se]$ MO is doubled. The $DS1$ (2 bands) charge has a bonding character for both P-Se and P-P. The $DS2$ (2 bands) charge presents bonding P-Se and antibonding P-P character. The $DS3$ (eight bands) charge has a bonding character for P-Se and antibonding for P-P. It is located mainly on Se atoms and it is polarized toward the neighbor P atoms. The $DS4$ (two bands) charge is mainly concentrated on the P atoms. It has a bonding character for P-P and antibonding for P-Se. The $DS5$ (2 bands) charge has antibonding character for both P-P and P-Se.

The electronic charge corresponding to the next four bands, labeled as $DS6$, belongs to the Sn[5s] AO with a small hybridization of some Se AO's. It presents a bonding character for Sn-Se.

The $DS7$ (ten bands) charge corresponds to the $4Sn[5p]$ AO and $6(P[3p]+3Se[4p])$ MO. The $Sn[5p]$ electrons have been partially transferred to the Se atoms, thus ensuring the ionic character of the structure. The remaining $Sn[5p]$ electrons have been concentrated in some distorted p lobes away from the Se electron clouds. Their orientation is almost perpendicular to the Sn-Se bond direction. Within the $[P_2Se_6]$ group the $Se[4p]$ orbitals are perpendicular to the

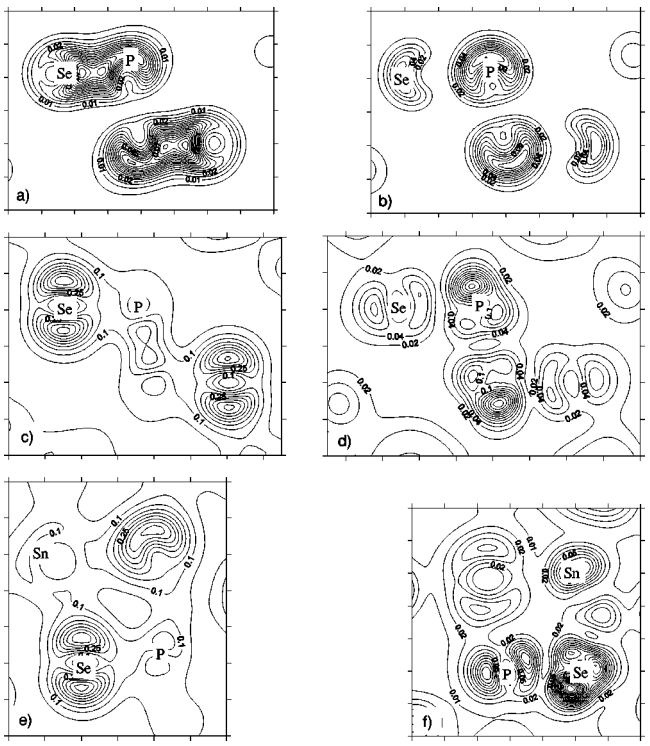

FIG. 4. Partial valence electron densities corresponding to different blocks of electronic bands of $Sn_2P_2Se_6$. (a)–(d) Transverse cross section through the $[P_2Se_6]$ group corresponding in order to the $DS2$, $DS5$, $DS8$, and $DS9$. (e) and (f) Cross sections passing through Sn-Se-P atoms corresponding to $DS8$ and $DS9$, respectively. The electronic charge belonging to the first two blocks stems mainly from P+Se electrons, while that of the $DS8$ block, the last valence block, stems mainly from Se+P atoms with a weak participation of Sn electrons. The block $DS9$, the first conduction block, contains hybrids belonging to all the three atoms. Line contours are in 0.005, 0.01, 0.05, and 0.02 $e/Å^3$ for $DS2$, $DS5$, $DS8$, and $DS9$, respectively. The side ticks are spaced by 2 bohrs.

P-Se bond direction, while the P$[3p]$ orbitals are very polarized towards Se. The $DS7$ charge has a bonding character for P-Se and P-P and an antibonding for Sn-Se.

The remaining 24 bands of the valence bands form a group labeled as $DS9$. The corresponding charge belongs mainly to the Se$[4p]$ AO's with some participation of P$[3p]$ AO's and less important Sn AO's. It presents a bonding P-P character and an antibonding P-Se character. The p lobes of Se are clearly seen.

The first bands in the conduction states ($DS10$) are p-type AO's which belong to all the three atoms. They present antibonding character for all P-P, P-Se, and Sn-Se.

V. STRUCTURAL RELAXATION

The *ab initio* determination of the crystal structure was done using a $2\times2\times2$ and a $4\times4\times4$ grid of special **k** points, with 2 and 16 **k** points in the irreducible part of the Brillouin zone, respectively. During the calculations a maximum limit of 10^{-5} hartree/bohr tolerance on the maximal force on the atoms is allowed. The results between the two grids of **k** points are very similar, with differences less than 1%. A further calculation using the theoretical structure and a grid of $6\times6\times6$ special **k** points, with 54 **k** points in the irreducible part of the Brillouin zone, showed that the residual axial stresses are lower than 10^{-5} hartree/bohr^3, the shear stresses are less than 10^{-6} hartree/bohr^3, and the forces on the atoms are less than 10^{-4} ha/bohr.

The results of the *ab initio* structural determination are presented in Tables I, II, and III.

TABLE I. *Ab initio* structural determination. Unit cell parameters.

Parameter	Experimental[a]	Theory	Difference (%)
a(Å)	6.8145	6.496	−4.67
b(Å)	7.7170	7.490	−2.93
c(Å)	11.692	10.955	−6.32
β(°)	124.54	124.84	0.68
$Volume$(Å^3)	506.473	437.473	−13.62

[a]Experimental parameters are taken from Ref. 21.

TABLE II. *Ab initio* structural determination. Atomic positions.

Atomic position	Experimental[a]	Theory	Difference (absolute)
Sn1_x	0.4917	0.4871	−0.0046
Sn1_y	0.1215	0.1291	0.0076
Sn1_z	0.6794	0.6800	0.0006
Sn2_x	0.0486	0.0637	0.0151
Sn2_y	0.3689	0.3659	−0.0030
Sn2_z	0.1753	0.1953	0.0200
P1_x	0.4179	0.4304	0.0125
P1_y	0.6424	0.6436	0.0012
P1_z	0.5222	0.5223	0.0001
P2_x	0.1670	0.1506	−0.0164
P2_y	0.8537	0.8524	−0.0013
P2_z	0.3917	0.3858	−0.0059
Se1_x	0.1799	0.1862	0.0063
Se1_y	0.4434	0.4366	−0.0068
Se1_z	0.5119	0.5146	0.0027
Se2_x	0.5864	0.5975	0.0111
Se2_y	0.5509	0.5531	0.0022
Se2_z	0.4200	0.4087	−0.0113
Se3_x	0.6689	0.6988	0.0299
Se3_y	0.7595	0.7783	0.0188
Se3_z	0.7253	0.7346	0.0093
Se4_x	0.3969	0.3872	−0.0097
Se4_y	0.0592	0.0660	0.0068
Se4_z	0.4025	0.3942	−0.0083
Se5_x	0.0089	0.9982	−0.0107
Se5_y	0.9451	0.9462	0.0011
Se5_z	0.5005	0.5079	0.0074
Se6_x	0.9148	0.8818	−0.0330
Se6_y	0.7441	0.7203	−0.0238
Se6_z	0.1859	0.1711	−0.0148

[a]Experimental parameters are taken from Ref. 21.

TABLE III. *Ab initio* structural determination. Bond lengths and angles. The labeling of the atoms corresponds to Fig. 1.

Parameter	Experimental [a]	Theory	Difference (%)
$[P_2Se_6]$ group			
P1-Se1 (Å)	2.1866	2.1828	−0.17
P1-Se2 (Å)	2.1912	2.1964	0.24
P1-Se3 (Å)	2.1852	2.2012	0.73
P1-P2 (Å)	2.2252	2.2121	−0.59
P2-Se4 (Å)	2.1819	2.1849	0.14
P2-Se5 (Å)	2.1981	2.1860	−0.55
P2-Se6 (Å)	2.1839	2.1977	0.63
Se1-P1-Se2 (deg)	110.20	110.40	0.18
Se1-P1-Se3 (deg)	116.69	119.07	2.04
Se2-P1-Se3 (deg)	113.37	113.25	−0.11
P2-P1-Se1 (deg)	102.67	100.22	−2.39
P2-P1-Se2 (deg)	107.37	108.63	1.17
P2-P1-Se3 (deg)	105.41	103.66	−1.66
P1-P2-Se4 (deg)	104.22	101.77	−2.35
P1-P2-Se5 (deg)	106.04	107.43	1.31
P1-P2-Se6 (deg)	106.87	104.72	−2.01
Se4-P-Se5 (deg)	107.74	107.03	−0.66
Se4-P-Se6 (deg)	115.83	115.86	0.03
Se5-P-Se6 (deg)	115.11	118.51	2.95
Selected Sn-Se bonds			
Sn1-Se1	3.1307	2.8914	−7.64
Sn1-Se2	3.5586	3.2251	−9.37
Sn1-Se3	2.9690	2.8657	−3.48
Sn1-Se4	2.9598	2.8513	−3.67
Sn1-Se5	3.0409	2.9457	−3.13
Sn1-Se4$(0\bar{1}0)$	3.3286	3.1305	−5.95
Sn2-Se1	2.9135	2.9221	0.29
Sn2-Se2	3.4201	3.1925	−6.65
Sn2-Se4	3.3545	2.9959	−10.68
Sn2-Se5	3.0816	2.9774	−3.38
Sn2-Se6	3.0591	2.8742	−6.04
Sn2-Se1$(0\bar{1}0)$	3.5539	3.1573	−11.16

[a]Experimental parameters are taken from Ref. 21.

The values of the unit cell parameters (Table I) are, as often observed in the LDA, smaller than the experimental ones. The difference is more important in the (010) plane that was subjected to an average compression of 5%. Still the β angle changes very little. The total volume contraction is significant: −13% with respect to the experiment. However, the atomic reduced coordinates (Table II) are in good agreement with the experiment, with absolute differences up to 0.03.

Table III shows that the theoretical geometry of the $[P_2Se_6]$ group agrees well with the experiment. The absolute differences in the calculated and experimental P-Se and P-P bond distances are less than 1% and the Se-P-Se angles are well described. The distortions between the two Se planes and the P-P bond direction are more important, as seen in the Se-P-P angle deviation from experiment.

The Sn-Se bond distances are worse. They are underestimated by the theory up to 10%. This underestimation comes from the weak bondings between the Se and the $[P_2Se_6]$ group, and looks very similar to the case of van der Waals bonding. This underestimation in the bond length accommodates the general underestimation of the volume, while preserving the experimental geometry of the $[P_2Se_6]$ group.

This underestimation suggests the need for the general gradient approximation (GGA),[30,31] which offers usually a better agreement with the experiment. Actually, preliminary data obtained from GGA calculations of the LDA-relaxed structure show relatively large stresses, on the order of $\sim -2.7\times10^{-4}$ hartree/bohr^3, and large forces, usually on the order of $\sim 5\times10^{-3}$ hartree/bohr, but raising up to $\sim 10^{-1}$ hartree/bohr for some of the Se atoms. The LDA underestimation is certainly due to the weak bonding between the $[P_2Se_6]$ group and the Sn cations, but it looks very similar to the known problems for the description of weak bonding in LDA (e.g., van der Waals).[32,33]

VI. BORN EFFECTIVE CHARGES

We computed the Born effective charges $Z^*_{\kappa,\alpha\beta}$, defined as the change in polarization due to an atomic displacement under zero external electric field. Table IV lists the calculated Born effective charges and the diagonal values. The Sn charges are weakly anisotropic, due to the neighbor Se atoms distributed evenly around the Sn atoms. The P and Se charges are much more anisotropic. The *x* and *y* components are higher than the *z* components, a fact which reflects the topology of the chemical bonds in the structure: the P_2Se_6 groups are linked by bridging Se-Sn-Se in all the three *x*, *y*, and *z* directions. But along both *x* and *y* directions the bonds are shorter than along the *z* direction. Consequently the polarization current that may flow along the *x* and *y* directions is more important than the one flowing along the *z* direction. There is no report of Born effective charge computations in $Sn_2P_2Se_6$. However for the isostructural $Sn_2P_2S_6$ compound, the effective charges calculated using Hartree-Fock techniques[6] (from 0.21 to 1.48 for P and from −0.74 to −1.16 for S) are very similar to our results.

On this basis the spontaneous polarization has been estimated using the first-order approximation, like in Refs. 34–36. For this purpose the spontaneous polarization along the direction β is approximated as the sum over all the atoms κ of the displacements along direction α multiplied by the corresponding $\alpha\beta$ component of the atomic Born effective charge tensor Z^*_κ, times the inverse of the unit cell volume Ω_0:

$$\delta P_\beta = \frac{1}{\Omega_0}\,\delta\tau_{\kappa,\alpha} Z^*_{\kappa,\alpha\beta}. \tag{1}$$

We compute the atomic displacements in the ferroelectric phase as the difference with respect to their corresponding positions in the paraelectric phase. Moreover, in the paraelectric phase there are two positions for the Sn atoms, denoted by Sn11 and Sn12,[21] and thus there are two possible

TABLE IV. Computed Born effective charges. The eigenvectors are given in brackets. The nominal charges of Sn, Se, and $[P_2Se_6]$ are 2, −2, and −4, the P nominal charge is −2, and the nominal charge for the group is −8. In the tensorial notation of the Born effective charges, the columns (lines) correspond to atomic displacements (polarization) directions.

Sn1	3.8821 0.1512 −0.0445
	0.4097 4.8634 0.0714
	0.0130 0.6425 4.7438
	[3.7941 4.4968 5.1983]
Sn2	4.1945 −0.0699 −0.4376
	0.3273 4.8622 −0.2756
	−0.0696 0.4386 4.9599
	[4.0902 4.8797 5.0466]
P1	2.2374 0.8563 −0.1287
	1.1738 1.9091 0.9346
	−0.3277 0.1801 1.1816
	[0.5309 1.6760 3.1212]
P2	1.4716 0.5952 −0.0792
	1.1829 1.8657 0.6551
	−0.6900 0.3578 1.9492
	[0.4943 2.1630 2.6292]
Se1	−1.8749 0.3198 0.7099
	−0.3561 −3.1747 −0.0460
	0.8820 0.2548 −1.8710
	[−1.0752 −2.6546 −3.1908]
Se2	−2.1646 −0.4889 −0.5756
	−0.4124 −1.6211 0.1412
	−0.4757 0.4323 −3.1424
	[−1.2257 −2.3267 −3.3757]
Se3	−2.2925 0.7323 0.0998
	0.9285 −2.0367 0.0480
	−0.2301 0.2400 −1.1158
	[−1.0863 −1.3431 −3.0156]
Se4	−1.4019 0.2829 0.7649
	−0.6865 −2.8011 −0.0343
	1.1027 0.1543 −2.5068
	[−0.8584 −2.7362 −3.1153]
Se5	−1.9559 −1.0541 −0.3883
	−0.7508 −1.9041 0.2359
	0.0492 0.4043 −2.8989
	[−0.9645 −2.7785 −3.0159]
Se6	−2.1751 0.7694 0.0851
	0.9336 −1.8699 0.3051
	−0.2479 0.2729 −1.2792
	[−1.0267 −1.3722 −2.9252]

choices for the calculation of the Sn displacements. We calculate first the displacements of the atoms as the difference between the *experimentally* determined low-T and high-T structures. Considering the Sn in the high-T structure in the Sn11 positions we obtain a spontaneous polarization of 22.56 μC/cm^2, corresponding to a [8.29 0.0 −20.98] μC/cm^2 Cartesian vector. Considering the Sn in the high-T structure in the Sn12 positions we obtain a slightly higher spontaneous polarization, of 23.44 μC/cm^2, corresponding to a [9.36 0.0−21.48] μC/cm^2 Cartesian vector. Then we repeat the same calculation taking the displacements of the atoms as the difference between the *calculated* low-T and experimentally determined high-T structures. We consider the Sn first in the Sn11 and second in the Sn12 positions and we obtain a spontaneous polarization of 14.87 and 15.93 μC/cm^2, corresponding to a [9.19 −0.0 −11.64] and [10.27 −0.0 −12.14] μC/cm^2 Cartesian vector, respectively.

To our knowledge there are no experimental measurements of the spontaneous polarization in $Sn_2P_2Se_6$ at low temperatures. However, it is possible to do a comparison with the experiment for some other structurally related compounds.[37] The $Sn_2P_2S_6$ has a spontaneous polarization of $\sim$15–16 μCcm^{-2}, according to Ref. 38. As the two compounds, which form a complete solid solution, exhibit many common physical properties, our results confirm this tendency. The spontaneous polarization of the ferrielectric $CuInP_2S_6$ is much lower,[39] $\sim 3\ \mu C\,cm^{-2}$, than for $Sn_2P_2S_6$ (experimental data) and $Sn_2P_2Se_6$ (this study).

VII. CONCLUSIONS

A first-principles study of the ferroelectric low-temperature phase of $Sn_2P_2Se_6$ was done using the local density approximation of density functional theory. The valence charge density was first determined; then the electronic band structure and the density of states were calculated.

An analysis of the different groups of electronic bands revealed the existence of isolated Sn orbitals and P-Se molecular orbitals. Thus, the main characteristic of the structure is the presence of a $[P_2Se_6]$ group, characterized by strong molecular bonds. The Sn^{2+} cations are ionically bonded with this group.

The *ab initio* determination of the structure in the LDA framework underestimates the total volume. This underestimation acts mainly on the Sn-Se interatomic bond distances, while the $[P_2Se_6]$ group is well described. However, the use of the GGA is suggested.

The calculated Born effective charges are relatively isotropic for Sn and highly anisotropic for P and Se. The spontaneous polarization is on the order of $\sim 15\ \mu C\,cm^{-2}$.

ACKNOWLEDGMENTS

Part of this research has been supported by FRFC Project No. 2.4556.99. R.C. thanks Y. Vysochanskii for a useful exchange of information. X.G. acknowledges financial support from the FNRS.

[1] M.M. Maior, S.A.J. Wiegers, Th. Rasing, S.W.H. Eijt, F.C. Penning, Y.M. Vysochanskii, S.F. Motrija, and H. van Kempen, Ferroelectrics **202**, 139 (1997).
[2] Y.M. Vysochanskii, Ferroelectrics **218**, 275 (1998).
[3] K. Moriya, H. Kuniyoshi, K. Tashita, Y. Ozaki, S. Yano, and T. Matsuo, J. Phys. Soc. Jpn. **67**, 3505 (1998).
[4] Y.M. Vysochanskii, A.A. Molnar, V.A. Stephanovich, V.B. Cajipe, and X. Bourdon, Ferroelectrics **226**, 243 (1999).
[5] P.P. Guranich, P.M. Lukach, V.V. Tovt, E.I. Gerzanich, A.G. Slivka, V.S. Shusta, and V.M. Kedyulich, Phys. Solid State **41**, 1166 (1999).
[6] M.B. Smirnov, J. Hlinka, and A.V. Solov'ev, Phys. Rev. B **61**, 15 051 (2000).
[7] S.W.H. Eijt and M.M. Maior, J. Phys.: Condens. Matter **60**, 4811 (1999).
[8] S.W.H. Eijt, M.M. Maior, and Y.M. Vysochanskii, Ferroelectrics **185**, 237 (1996).
[9] D. Baltrunas, A.A. Grabar, K. Mazeika, and Y.M. Vysochanskii, J. Phys.: Condens. Matter **11**, 2983 (1999).
[10] D. Baltrunas, K. Mazeika, Y.M. Vysochanskii, A.A. Grabar, and V.Y. Slivka, Ferroelectrics **165**, 359 (1995).
[11] S.W.H. Eijt, Ph.D. thesis, Katholieke Universiteite Nijmegen, Nijmegen, Holland, 1997.
[12] S.W.H. Eijt, R. Currat, J.E. Lorenzo, P. Saint-Gregoire, B. Hennion, and Y.M. Vysochanskii, Eur. Phys. J. B **5**, 169 (1998).
[13] S.W.H. Eijt, R. Currat, J.E. Lorenzo, P. Saint-Gregoire, S. Katano, T. Janssen, B. Hennion, and Y.M. Vysochanskii, J. Phys.: Condens. Matter **10**, 4811 (1998).
[14] M.M. Maior, P.H.M. van Loosdrecht, H. van Kempen, Th. Rasing, S.B. Molnar, and S.F. Motrij, J. Phys.: Condens. Matter **5**, 6023 (1993).
[15] M.M. Maior, Th. Rasing, S.W.H. Eijt, P.H.M. van Loosdrecht, H. van Kempen, S.B. Molnar, Y.M. Vysochanskii, S.F. Motrij, and V.Y. Slivka, J. Phys.: Condens. Matter **6**, 11 211 (1994).
[16] A. Drobnich and Y. Vysochanskii, Ferroelectrics **226**, 37 (1999).
[17] Y.M. Vysochanskii and A.V. Drobnich, Ferroelectrics **236**, 105 (2000).
[18] P. Hohenberg and W. Kohn, Phys. Rev. **136**, B864 (1964).
[19] W. Kohn and L.J. Sham, Phys. Rev. **140**, A1133 (1965).
[20] X. Gonze, R. Caracas, P. Sonnet, F. Detraux, P. Ghosez, I. Noiret, and J. Schamps, in *Fundamental Physics of Ferroelectrics 2000*, edited by Ronald E. Cohen, AIP Conf. Proc. No. 535 (AIP, Melville, NY, 2000), pp. 13–20; url: http://www.mapr.ucl.ac.be/ABINIT/.
[21] R. Israel, S.W.H. Eijt, R. de Gelder, J.M.M. Smiths, P.T. Beurskens, Th. Rasing, H. Van Kempen, M.M. Maior, and S.F. Motrija, Z. Kristallogr. **213**, 34 (1998).
[22] R. Enjalbert, J. Galy, Y. Vysochanskii, A. Ouedraogo, and P. Saint-Gregoire, Eur. Phys. J. B **8**, 169 (1999).
[23] M.C. Payne, M.P. Teter, D.C. Allan, T.A. Arias, and J.D. Joannopoulos, Rev. Mod. Phys. **64**, 1045 (1992).
[24] X. Gonze, Phys. Rev. B **54**, 4383 (1996).
[25] N. Troullier and J.L. Martins, Phys. Rev. B **43**, 1993 (1991).
[26] H.J. Monkhorst and J.D. Pack, Phys. Rev. B **13**, 5188 (1976).
[27] W.H. Press, B.P. Flannery, S.A. Teukolsky, and W.T. Vetterling, *Numerical Recipes: The Art of Scientific Computing (FORTRAN Version)* (Cambridge University Press, Cambridge, England, 1989).
[28] X. Gonze, Phys. Rev. B **55**, 10 337 (1997).
[29] X. Gonze and C. Lee, Phys. Rev. B **55**, 10 355 (1997).
[30] J.P. Perdew and Y. Wang, Phys. Rev. B **45**, 13 244 (1992).
[31] J.A. White and D.M. Bird, Phys. Rev. B **50**, 4954 (1994).
[32] R.O. Jones and O. Gunnarsson, Rev. Mod. Phys. **61**, 689 (1989).
[33] Y. Andersson, D.C. Langreth, and B.I. Lundqvist, Phys. Rev. Lett. **76**, 102 (1996).
[34] W. Zhong, D. Vanderbilt, and K.M. Rabe, Phys. Rev. Lett. **73**, 1861 (1994).
[35] W. Zhong, D. Vanderbilt, and K.M. Rabe, Phys. Rev. B **52**, 6301 (1995).
[36] L. Bellaiche, A. Garcia, and D. Vanderbilt, Phys. Rev. Lett. **84**, 5427 (2000).
[37] M.M. Khoma, A.A. Molnar, and Y.M. Vysochanskii, J. Phys. Stud. **2**, 524 (1998).
[38] Y.M. Vysochanskii, A.A. Molnar, M.M. Khoma, and S.F. Motrija, Condens. Matter Phys. **2**, 421 (1999).
[39] Y.M. Vysochanskii, V.A. Stephanovich, A.A. Molnar, V.B. Cajipe, and X. Bourdon, Phys. Rev. B **58**, 9119 (1998).